Conformational Changes in the N-Terminal Region of Photoactive Yellow Protein: A Time-Resolved Diffusion Study

Yuji Hoshihara,* Yasushi Imamoto,† Mikio Kataoka,‡ Fumio Tokunaga,§ and Masahide Terazima*
*Department of Chemistry, †Department of Biophysics, Graduate School of Science, Kyoto University, Kyoto 606-8502, Japan; ‡Graduate School of Materials Science, Nara Institute of Science and Technology, Nara 630-0192, Japan; and §Department of Earth and Space Science, Graduate School of Science, Osaka University, Toyonaka, Osaka 560-0043, Japan

ABSTRACT The kinetics of conformational change in the N-terminal region of photoactive yellow protein (PYP) was studied by the time-resolved diffusion measurement. The transient grating signal that represented the protein diffusion of the ground state and pB state depended on the observation time range. An analysis of the signal based on the time-dependent diffusion coefficient clearly showed that protein diffusion changed with a time constant of 170 μs, corresponding to the $pR_2 \rightarrow pB'$ transition. Since a previous diffusion study of N-terminal truncated PYPs had revealed that the change in the diffusion coefficient reflected the unfolding of the α-helices in the N-terminal region of PYP, the results indicate that this unfolding took place at the same rate as the $pR_2 \rightarrow pB'$ transition. This demonstrates that the response of the conformational change in the N-terminal region was quite fast, probably due to changes in a specific hydrogen-bonding network of this domain.

INTRODUCTION

Conformational change in proteins is a key step in signal transduction. For understanding the molecular mechanism of such changes, it is essential to reveal their dynamics in the time domain. For clarifying the relationship between reaction kinetics and conformational change, photoactive yellow protein (PYP), a relatively small (14 kDa) water-soluble protein presumably functioning as a blue light photoreceptor for a negative phototactic response, has been used as a prototype system by taking advantage of light triggering (1–12). We investigated a reaction step that changed the conformation of the N-terminal region of PYP by applying a unique technique—time-resolved diffusion measurement.

The chromophore in PYP is *p*-coumaric acid (4-hydroxycinnamic acid) covalently bound to the side chain of Cys-69 via a thioester linkage (3,5). After photoexcitation of the chromophore, the photocycle of PYP is triggered by *trans-cis* photoisomerization, which has been characterized mostly by the flash photolysis method (6–8). Upon flash excitation, the ground state (pG) is converted to a red-shifted intermediate pR_1 (I_1 or PYP_L) in <2 ns (9). Subsequently, pR_1 is converted to pR_2 without the spectral change with a time constant of ~ 1 μs (10). The pR_2 species decays on the submillisecond timescale to a blue-shifted intermediate pB′ (or I_2 or $PYP(M)_{acid}$), which is converted to pB (or I_2' or $PYP(M)_{alkali}$) within a few milliseconds at room temperature. This pB finally returns to pG within a few seconds (2,4,9).

The conformational changes of PYP have been examined by a variety of techniques (13–23). A study using the hydrophobic probe molecule Nile red indicated that exposure of the hydrophobic surface, which is a part of the chromophore-binding pocket, followed protonation of the chromophore (14). A hydrogen/deuterium exchange study suggested instability of the conformation in the N-terminal region and large structural changes in the protein backbone, involving both solvent-accessible and core regions upon the formation of pB (15,16). Furthermore, the thermodynamic properties of the transition state also suggested the unfolding of the N-terminal region (17). Far-ultraviolet circular dichroism (CD) and Fourier transform infrared (FTIR) studies of N-terminal truncated PYPs suggested conformational changes of α-helices and β-sheets, respectively (13). Recently, an NMR structure of a PYP lacking 25 N-terminal residues (Δ25) was reported (18) showing that the central β-sheet and a small part of one α-helix in the helical connector region were still intact but that the remainder was highly flexible in the pB state. Conformational change was also detected by monitoring the diffusion coefficient (D) of the intermediate species, pB (19,20). It was reported that D of pB (D_{pB}) was smaller than D of pG (D_{pG}) (21). The smaller D_{pB} was attributed to a significant conformational change that increased the friction for translational diffusion (a diffusion-sensitive conformational change). A later study on certain N-terminal truncated PYPs concluded that the conformational change at the N-terminal region was the main cause of the change in D and that the solvation structure around this group was significantly altered (20). Hence, the reduction in D was explained in terms of the increase in intermolecular interactions upon the unfolding of the α-helices in the N-terminal region. It should be noted here that ''unfolding of the α-helices'' does not necessarily mean the formation of a random coil or stretched structure of the N-terminal region. The observed changes in D indicated that the intramolecular hydrogen-bonding network in the α-helices was changed to protein-water intermolecular hydrogen bonding. However, it was reasonable to

Submitted June 15, 2007, and accepted for publication October 31, 2007.

Address reprint requests to Masahide Terazima, E-mail: mterazima@kuchem.kyoto-u.ac.jp.

Editor: Janos K. Lanyi.

0006-3495/08/03/2187/07 $2.00

doi: 10.1529/biophysj.107.115253

assume that the conformation was no longer α-helices without this intramolecular hydrogen bonding.

Despite these extensive investigations, kinetic studies of the conformational change in solution have been rather limited. A time-resolved infrared (IR) study revealed that the protonation of *p*-coumaric acid and Glu-46 ionization occurred with a time constant of 260 μs ($pR_2 \rightarrow pB'$) and that conformational change of the C=O stretch of the protein backbone (amide I) in the antiparallel β-sheet took place later with a time constant of 2 ms ($pB' \rightarrow pB$) (24). However, kinetic information on the conformational change in the N-terminal region has not yet been detected. For example, the structural change of the hydrophobic surface shielded by the N-terminus was not observed by the Nile red binding technique (14).

In this study, we successfully obtained kinetic parameters of the conformational change in the N-terminal region by using the time-resolved diffusion measurement. Although D has been categorized as a steady-state characteristic so far, it was demonstrated recently that this property can be used to characterize the conformation of unstable intermediate species during a reaction in real time by the pulsed laser induced transient grating (TG) technique (20,25–32). For example, it was reported that D of unfolded cytochrome *c* gradually increased in conjunction with the protein folding process (25). This change was attributed to the helices formation, along with a change in the hydrogen-bonding network from intermolecular to intramolecular bonding. Spectrally silent conformational dynamics of the LOV (light-oxygen-voltage sensing) domain of a phototropin was investigated using the time dependence of D, showing that it decreased with a time constant of 2 ms (26,28). The change in D was explained in terms of the unfolding of the α-helices at this rate. Spectrally silent dynamics of photosensor proteins have also been detected (27,29–31). However, such a time-dependent D has not been observed for the PYP reaction so far in the time window (5–100 ms) achievable with the grating wavenumber (q) normally used in our group ($1 \times 10^{11}\ m^{-2} < q^2 < 2 \times 10^{12}\ m^{-2}$) (21). The time independence of D in this time window indicated that the change in D was complete within a few milliseconds. For monitoring this change on a shorter timescale than before, the TG signal should be recorded at large q, which was rather difficult. In this study, using a careful alignment of the experimental setup, we succeeded in recording the diffusion signal in the submillisecond range. We analyzed the observed TG signals over a wide time range for time-dependent changes in D and concluded that conformational changes in the N-terminus took place with a time constant of 170 μs, which corresponded to the rate of formation of pB' under the experimental conditions. Hence, this result indicated that the conformation of the N-terminus changed during an early step of the reaction, before changes occurred in the structure of the chromophore binding domain previously monitored by the FTIR method (24). To our knowledge, this is the first report on the kinetics of the conformational change in the N-terminal region.

THEORY

The principle of the TG measurement has been reported previously (32,33). The TG signal intensity is proportional to the square of the light-induced refractive index change (δn) as long as the absorption change is negligible at the probe wavelength, which was satisfied under these experimental conditions. There are two main contributions to the refractive index change: the thermal effect ($\delta n_{th}(t)$, thermal grating) and change in chemical species upon reaction ($\delta n_{spe}(t)$, species grating). The species grating signal intensity is given by the difference between the refractive index changes due to the reactant (δn_R) and the product (δn_P). Hence, the TG signal ($I_{TG}(t)$) can be expressed as

$$I_{TG}(t) = \alpha\{\delta n_{th}(t) + \delta n_P(t) - \delta n_R(t)\}^2, \quad (1)$$

where α is a constant. The ''product'' in this equation does not necessarily mean the final product but can be any molecule produced from the reactant at the observation time. The negative sign of δn_R is due to the depletion of the reactant.

When the molecular diffusion coefficient (D) is time independent, the temporal profile of the species grating signal can be calculated by the molecular diffusion equation, and we may find that the q-Fourier component of the concentration decays with a rate constant of Dq^2 for the reactant and the product. (In principle, the molecular diffusion and thermal diffusion are coupled. However, the coupling is generally very weak; so we can neglect this coupling as shown by a number of reports (19–22,25–35).) Hence, the time development of the TG signal for describing the molecular diffusion part can be expressed by

$$I_{TG}(t) = \alpha\{\delta n_P^0 \exp(-D_P q^2 t) - \delta n_R^0 \exp(-D_R q^2 t)\}^2, \quad (2)$$

where D_R and D_P are diffusion coefficients of the reactant and the product, respectively. Furthermore, $\delta n_R^0 (>0)$ and $\delta n_P^0 (>0)$ are the initial refractive index changes due to the changes in the reactant and the product concentrations, respectively, upon the reaction.

When D changed in this observation time window, the kinetics must be included in the diffusion equation. In this study, we examined the following two possible schemes for changes in D:

$$pR_2\,(D_{pG}) \xrightarrow{k_1} pB'\,(D_{pB}) \xrightarrow{k_2} pB\,(D_{pB}) \quad \text{(Scheme 1)}$$

$$pR_2\,(D_{pG}) \xrightarrow{k_1} pB'\,(D_{pG}) \xrightarrow{k_2} pB\,(D_{pB}), \quad \text{(Scheme 2)}$$

where D_{pG} and D_{pB} represent D of the initial (pG) and the final (pB) species, respectively. Scheme 1 represents the change in D for the transition from pR_2 to pB' with a rate constant of k_1, which was 170 μs at room temperature in this study. Scheme 2 depicts the change in D for the transition from pB' to pB with a rate constant of k_2, which was 1 ms. Solving the diffusion equations, which are similar to those reported before (32), with initial conditions of $[pR_2] =$

$[pR_2]_0(1 - \cos qx)$ (q: grating wavenumber, x: direction of the grating wave vector), $[pB'] = 0$, and $[pB] = 0$, the time dependence of the refractive indices for both cases are given by Scheme 1:

$$I_{TG} = \alpha\{(\delta n_{pR2} - \delta n_{pB'}k_1/(A+B) + \delta n_{pB}k_1/((-A-k_1)(-A-B)))\exp[-(D_{pG}q^2 + k_1)t] + (\delta n_{pB'}k_1/(A+B) + \delta n_{pB}k_1(-A-k_1)/((-A-k_1)(-A-B)))\exp[-(D_{pB}q^2 + k_2)t] + (\delta n_{pB}k_1(A+B)/((-A-k_1)(-A-B)))\exp(-D_{pB}q^2t) - \delta n_{pG}\exp(-D_{pG}q^2t)\}^2 \quad (3)$$

Scheme 2:

$$I_{TG} = \alpha\{(\delta n_{pR2} - \delta n_{pB'}k_1/B - \delta n_{pB}k_1k_2(-A-k_2)/((-A-k_1)(-A-k_2)B))\exp[-(D_{pG}q^2 + k_1)t] + (\delta n_{pB'}k_1/B - \delta n_{pB}k_1k_2(A-k_1)/((-A-k_1)(-A-k_2)B))\exp[-(D_{pG}q^2 + k_2)t] + (\delta n_{pB}k_1k_2B/((-A-k_1)(-A-k_2)B))\exp(-D_{pB}q^2t) - \delta n_{pG}\exp(-D_{pG}q^2t)\}^2, \quad (4)$$

where $A = D_1q^2 - D_2q^2$ and $B = (k_1 - k_2)$.

Equations 3 and 4 are different from the equation reported previously (21) because the previous equation did not consider the time dependence of D. The previous equation was sufficient to reproduce the observed TG signal before because the observation time range was slow enough (slower than the D-change dynamics).

MATERIALS AND METHODS

The experimental setup for the TG experiments was similar to that reported in previous studies (10,19–21,35). A XeCl excimer laser-pumped dye laser (Lambda Physik, Göttingen, Germany; Compex 102xc, Lumonics Hyper Dye 300; $\lambda = 465$ nm) beam was split into two by a beam splitter and crossed inside a quartz sample cell (optical path length = 2 mm) by a focusing lens. The laser power of the excitation was <5 μJ/pulse. The created refractive index modulation (TG) in the sample was probed by a He-Ne laser (633 nm) or a diode laser (840 nm) as a Bragg diffracted signal (TG signal). The grating wavenumber q was changed by changing the crossing angles of the excitation beams and the probe beam. For achieving a wide range of q, a variety of lenses with different focal lengths were used. The TG signal was detected by a photomultiplier tube (Hamamatsu R-928; Hamamatsu, Japan) and fed into a digital oscilloscope (Tektronix 2430A; Beaverton, OR). The TG signal was averaged by a microcomputer to improve the signal/noise ratio. All measurements were carried out at room temperature.

PYP was prepared as reported previously (10,21,35) and was dissolved in 10 mM Tris-HCl (pH = 8.0) with 0.5 mM PMSF (phenylmethanesulfonyl fluoride). Bromocresol purple was used as a calorimetric reference for the TG measurement. The absorbance at the excitation wavelength was ~0.4–0.7 in these experiments.

RESULTS

To determine the time dependence of the change in D, it was necessary to analyze the TG signals consistently over a wide q^2 range. The features of the TG signal of PYP will first be briefly described. The signal rose quickly after photoexcitation with the instrumental response of our system and then showed a weak slow-rising component (Fig. 7 in Takeshita et al. (10)). The latter component observed just after the photoexcitation was attributed to the protein conformational change from pR_1 to pR_2, without an accompanying change in the absorption spectrum of PYP. After this, the signal decayed to a certain intensity with a rate constant $D_{th}q^2$ and showed growth-decay curves twice before finally decaying to the baseline. The component with the decay rate constant of $D_{th}q^2$ must be the thermal grating component. A typical TG signal at $q^2 = 3 \times 10^{11}$ m^{-2} is shown in Figs. 1 *A* (*a*) and *B* (*a*). For simplicity, the signal after the thermal grating component is shown. The first growth component in this figure represents the transformation of pR_2 to pB. This kinetics was expressed by a biexponential function with a time constant of 170 μs and 1 ms at 293 K, which could be monitored by detecting absorption changes. The subsequent decay and the next growth-decay curve were attributed to the protein diffusion of pG and pB (10). This latest peak (diffusion peak) appeared because D_{pB} was different from D_{pG}. The diffusing species were assigned based on the signs of the refractive index changes, and it was concluded that the rate constant of the rising component represented $D_{pG}q^2$ and that of the decaying component corresponded to $D_{pB}q^2$ ($D_{pG} > D_{pB}$) (10). Hence, the observed TG signals after the thermal grating were reproduced well by

$$I_{TG}(t) = \alpha\{\delta n_{th}\exp(-D_{th}q^2t) + \delta n_1\exp(-k_1t) + \delta n_2\exp(-k_2t) - \delta n_{pG}\exp(-D_{pG}q^2t) + \delta n_{pB}\exp(-D_{pB}q^2t)\}^2, \quad (5)$$

where the rate constants k_1 and k_2 represent the $pR_2 \rightarrow pB$ kinetics, and the preexponential factors represent the refractive index changes. This equation was used to reproduce the previously observed TG signal (21). Here, the pR_1 and pR_2 formation processes were omitted to focus on the relation between the reaction kinetics of k_1, k_2, and the protein dif-

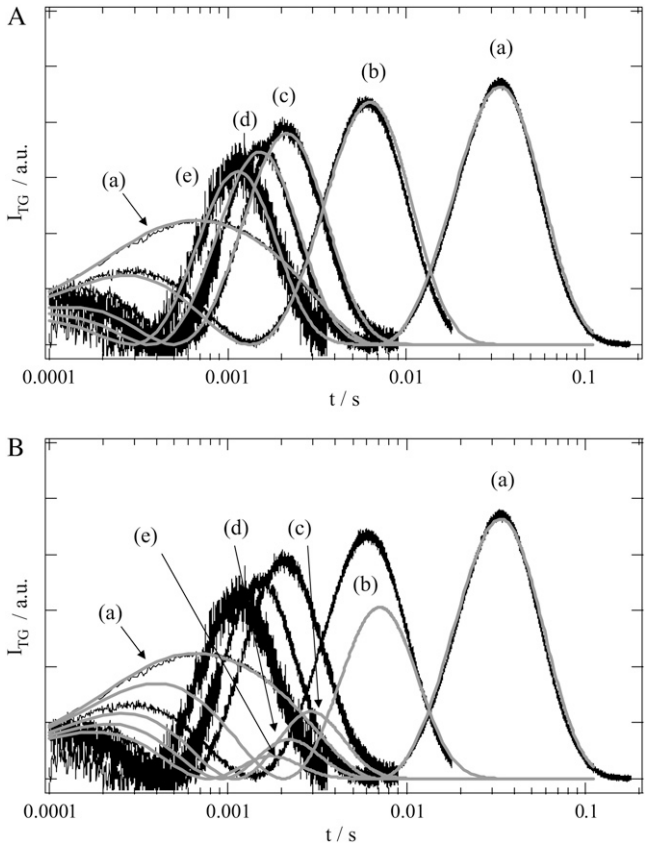

FIGURE 1 TG signals (*solid lines*) of PYP measured at q^2 of (*a*) 3×10^{11}, (*b*) 1.64×10^{12}, (*c*) 5×10^{12}, (*d*) 7.3×10^{12}, and (*e*) 1×10^{13} m^{-2}. The signals are normalized by the thermal grating intensities, not shown in this figure. (*A*) The calculated signals based on Scheme 1 (time constant = 170 μs) are shown by the gray lines. (*B*) The calculated signals based on Scheme 2 (time constant = 1 ms) (*gray lines*) are superimposed. The labels (*a–e*) in (*B*) indicate the calculated signals in this panel.

fusion processes. From the curve fitting of the signal, D_{pG} and D_{pB} were previously determined to be 1.35×10^{-10} m^2s^{-1} and 1.15×10^{-10} m^2s^{-1}, respectively (10).

Fig. 1 shows the TG signals measured over a wide range of q^2. These signals were normalized by the intensity of the thermal grating component, which was an indicator of the concentration of the photoexcited PYP. There were several interesting features in the signal. In particular, it is noted that the diffusion peak intensity decreased with increasing q^2, i.e., in the faster time region. If there was no change in D during the diffusion process, the time dependence would be expressed by a combination of $\exp(-Dq^2t)$ terms (e.g., Eq. 2). In this case, the diffusion peak intensity, which is determined by the difference of two exponential functions, should not be expected to depend on q^2. Since the diffusion peak appears to be due to the change in D of the intermediate species, the weaker diffusion peak intensity in the earlier time range is clear evidence for the smaller difference between D_P and D_R on a fast timescale. The time-dependent change in the diffusion signal intensity was attributed to the time-dependent decrease in the apparent D of the product, because D of the reactant (D_{pG}) should be constant. This finding prompted the efforts to determine the rate of change in D from these signals.

We examined two possible reaction schemes for explaining the observed signal at various values of q^2: the change in D associated with the transition from pR_2 to pB′ (Scheme 1: Eq. 3) or with the transition from pB′ to pB (Scheme 2: Eq. 4). To distinguish between these two routes, we used the following methods.

First, we tried to fit the temporal profiles of the signals at various q^2 consistently. For this purpose, we initially fit the signal at the lowest q^2 (Figs. 1 (*a*) and *B* (*a*)) with $D_{pG} = 1.35 \times 10^{-10}$ m^2s^{-1} and $D_{pB} = 1.15 \times 10^{-10}$ m^2s^{-1}, which were determined previously from the data at relatively low q^2; i.e., kinetics of change in D can be ignored in this long time range (20). Adjustable parameters of the fitting were the refractive index changes, δn_{pG}, δn_{pR2}, $\delta n_{pB'}$, and δn_{pB}. By properly adjusting these refractive index changes, the signal at $q^2 = 3 \times 10^{11}$ m^{-2} could be satisfactorily reproduced by both Eqs. 3 and 4 (Fig. 1, *A*(*a*) and *B*(*a*)). The reasonable fits based on both schemes are not surprising because the dynamics of the change in D were already complete at the diffusion peak time at this small q^2. We then calculated the TG signals at the larger q^2 using these parameters. Surprisingly, the calculated signals based on Scheme 1 reproduced the observed signals very well without the use of any adjustable parameters (Fig. 1 *A*). On the other hand, the calculated signal intensities based on Scheme 2 were drastically lower than the observed values at the higher q^2 (Fig. 1 *B*). Apparently, this difference comes from the different rates of change in D we used for these calculations. The very good reproduction without any adjustable parameter strongly suggested that Scheme 1 correctly described the change in D of PYP.

To further support this conclusion, we analyzed the peak times (t_{max}) of the diffusion signals at various q^2. The peak time was determined by the difference of two exponential functions that represented the diffusion of pG and the intermediate. Hence, it is natural that when q^2 is increased t_{max} decreases. However, if the D-change was complete in a fast time range (e.g., <50 μs), the temporal profile of the TG signal is determined by Eq. 2, and hence $t_{max}q^2$ should not depend on q^2. Fig. 2 depicts a plot of the experimentally determined $t_{max}q^2$ against q^2. Apparently, this $t_{max}q^2$ depended on q^2, clearly indicating the time dependence of D in this time window. We superimposed calculated $t_{max}q^2$ based on Schemes 1 and 2 on this plot. It is apparent that $t_{max}q^2$ calculated from Eq. 3 (Scheme 1) reproduces the observed times, whereas $t_{max}q^2$ from Eq. 4 (Scheme 2) does not. This analysis is a clear presentation showing that the D-change took place with a time constant of 170 μs, not 1 ms.

For further confirmation of the above treatment, we measured the TG signals of an N-terminal truncated PYP, which lacked the N-terminal 15 amino acid residues (T15). Previously, we reported that the D-change is smaller than that for the intact PYP, and the rate of $pR_2 \rightarrow$ pB′ became faster when

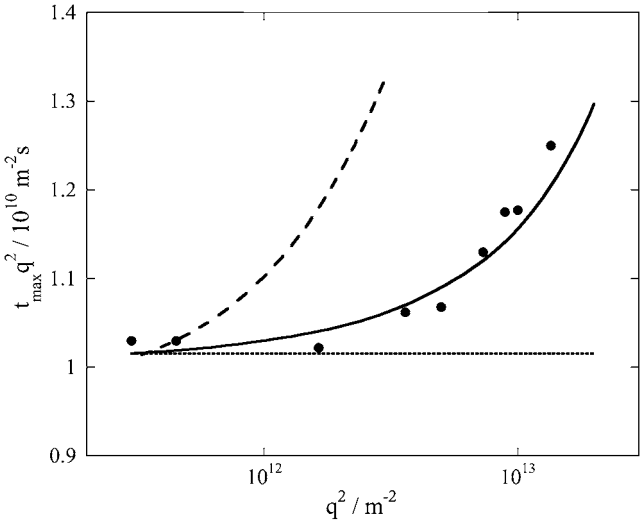

FIGURE 2 Plot of $t_{max}q^2$ against q^2 (*solid circles*). The calculated $t_{max}q^2$ based on Scheme 1 and Scheme 2 are shown by the solid line and the broken line, respectively. The calculated $t_{max}q^2$ without change in D is also shown by dotted line, which illustrates the lack of dependence on q^2.

the N-terminal region was eliminated (20). Fig. 3 depicts the observed TG signals at various q^2. Since the D-change for T15 is smaller, the diffusion peak intensity is weaker than that of the intact PYP. However, we could reproduce the signals by Eq. 3 with $D_{pG} = 1.27 \times 10^{-10}\ m^2s^{-1}$ and $D_{pB} = 1.15 \times 10^{-10}\ m^2s^{-1}$ (20) and a time constant of 50 μs, which were determined for the $pR_2 \rightarrow pB'$ rate from the population grating signal. This result supports the idea that the conformation change in the N-terminal region is quite fast.

DISCUSSION

A previous time-resolved IR study showed biphasic dynamics for the transition from pR_2 to pB (24). The faster phase

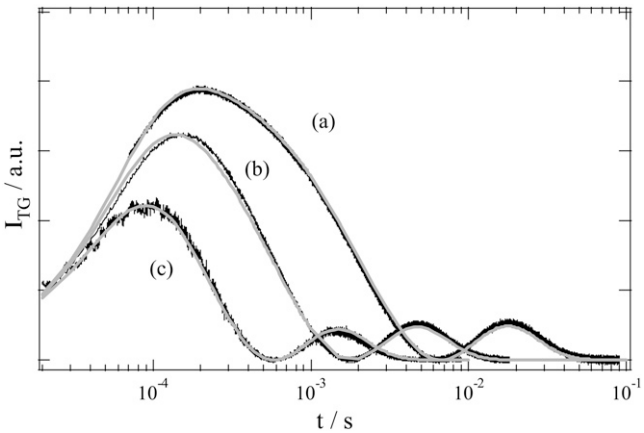

FIGURE 3 TG signals (*black lines*) of T15 measured at q^2 of (*a*) 7.5×10^{11}, (*b*) 2.8×10^{12}, and (*c*) $9.1 \times 10^{12}\ m^{-2}$. The signals are normalized by the thermal grating intensities, not shown in this figure. The calculated signals based on Scheme 1 (time constant = 50 μs) are shown by the gray lines.

($pR_2 \rightarrow pB'$) was assigned to the protonation of *p*-coumaric acid and Glu-46 ionization, whereas the slower phase ($pB' \rightarrow$ pB) involved global conformational changes in PYP (24). These conformational changes were attributed to the C=O stretch of the protein backbone (amide I) in the antiparallel β-sheet. In fact, an FTIR spectrum of an N-terminal truncated PYP showed a drastic change in amide I bands compared to intact PYP even for PYP possessing the α-helices in the N-terminal region (13). These studies indicated that it is rather difficult to discern the conformational changes in the N-terminal region from changes in the time-resolved FTIR spectra. A previous time-resolved optical rotatory dispersion experiment also showed that the dominant change occurred with a 2 ms time constant (23). However, the CD spectra of N-terminal truncated PYPs showed that the contributions of the N-terminal helices are not large in the total CD intensity (13). Hence, it is possible that the conformation change of the N-terminal could not be detected by the time-resolved CD either. On the other hand, it was previously shown that the diffusion-sensitive conformational change reflected the unfolding of the α-helices in the N-terminus (20). Therefore, the conclusion from this time-resolved D study should provide information on the kinetics of the conformational changes in this region.

It is interesting to note that the conformational change in the N-terminal region, which was monitored by the TG method, occurred with a time constant of 170 μs, whereas the time constant of the change in the β-sheet was reported to be 2 ms in the previous FTIR study (24). Furthermore, CD measurements at two different pHs showed that a significant change (36%) in the CD intensity, which was attributed to the unfolding of the α_3- and/or α_5-helices and disruption of the β-sheet of PYP_M^{alkali}, which may correspond to pB (36,37). A minor change (9%) in CD intensity observed in PYP_M^{acid}, which may be similar to pB′, could represent the unfolding of the α-helices in the N-terminal region. However, we should consider the fact that the reaction intermediates during the time-resolved measurements under the native condition may not be the same as the species observed under different pH conditions. Therefore, the changes in the β-sheet cannot be the cause of the unfolding of the α-helices in the N-terminal region. Rather, we propose that the conformational changes in the N-terminal region induce the changes in the β-sheet of the chromophore binding domain.

Since we did not observe any change in D with a time constant of 1 or 2 ms, we concluded that the conformational change in the chromophore binding domain does not change D. The D-insensitivity of the 1 or 2 ms conformational change that was previously observed by the FTIR or CD methods is not surprising if this conformational change does not induce the hydrogen-bonding network switching from the intramolecular to intermolecular bonding. Interestingly, these features are similar to those of other photosensor proteins, phototropin 1 (phot1) and phototropin 2 (phot2), which possess the LOV domains, a member of the Per-Arnt-Sim (PAS) family. After

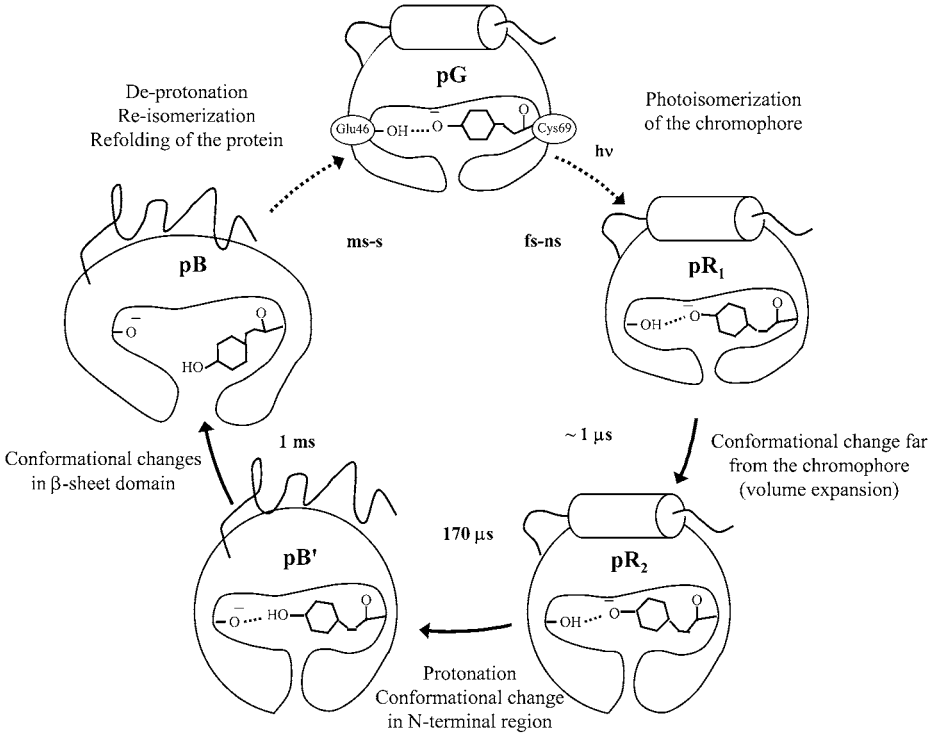

FIGURE 4 Schematic illustration of the conformation change in PYP.

light triggering in the LOV domain of phot1 and phot2, the α-helices in the linker region were unfolded and the diffusion became slower (26,28). On the other hand, the conformational change in the LOV domain does not change D. These observations indicate that the hydrogen-bonding networks in the PAS core (PYP and phototropins) are not altered by the photoexcitation, whereas the conformations of the region attached on the PAS core do change significantly.

It was of some interest to note that the conformational change in the N-terminus occurred with the same rate as the protonation of the chromophore. Recently, it was suggested that the α-helices in the N-terminal region were stabilized by the hydrogen-bonded network in the protein structure (38). We suggest that the protonation of the chromophore changed this network, causing unfolding of the α-helices in the N-terminal region. The fact that the time constant of the conformational change was equal to that of the protonation of the chromophore detected by FTIR indicated that these responses were very rapid.

CONCLUSION

Conformational changes of PYP upon photoexcitation were studied from a viewpoint of diffusion coefficient (D) in the time domain. The TG signals measured over a wide q^2 range were consistently fitted by the equation based on the change in D occurring with a time constant of 170 μs. On the other hand, the signals could not be reproduced at all by the equation based on a model for change in D with a time constant of 1 ms. Previously, we identified that this D-change reflected the conformational changes in the α-helices of the N-terminal region. Hence, we concluded that the α-helices at the N-terminal region is unfolded with 170 μs (pR_2-pB' process). In light of the previous time-resolved FTIR results (24), we concluded that the N-terminal α-helices changes faster than the conformation of the β-sheets in the chromophore-binding domain. This faster rate suggests that the N-terminal conformation is stabilized by a specific weak interaction, as suggested before (38), and that this interaction is perturbed by the protonation of the chromophore. The time response of the conformation in the N-terminal region is very fast. The reaction scheme of PYP is summarized in Fig. 4.

A part of this study was supported by the Grant-in-Aid (Nos. 13853002 and 15076204) from the Ministry of Education, Culture, Sports, Science, and Technology of Japan.

REFERENCES

1. Sprenger, W. W., W. D. Hoff, J. P. Armitage, and K. J. Hellingwerf. 1993. The eubacterium Ectothiorhodospira halophila is negatively phototactic, with a wavelength dependence that fits the absorption spectrum of the photoactive yellow protein. *J. Bacteriol.* 175:3096–3104.
2. Meyer, T. E., E. Yakali, M. A. Cusanovich, and G. Tollin. 1987. Properties of a water-soluble, yellow protein isolated from a halophilic phototrophic bacterium that has photochemical activity analogous to sensory rhodopsin. *Biochemistry.* 26:418–423.
3. Hoff, W. D., P. Düx, K. Hard, B. Devreese, I. M. Nugteren-Roodzant, W. Crielaard, R. Boelens, R. Kaptein, J. van Beeumen, and K. J. Hellingwerf. 1994. Thioester-linked *p*-coumaric acid as a new photo-

active prosthetic group in a protein with rhodopsin-like photochemistry. *Biochemistry*. 33:13959–13962.

4. Hellingwerf, K. J., J. Hendriks, and T. Gensch. 2003. Photoactive yellow protein, a new type of photoreceptor protein: will this ''yellow lab'' bring us where we want to go? *J. Phys. Chem. A*. 107:1082–1094.
5. Baca, M., G. E. O. Borgstahl, M. Boissinot, P. M. Burke, D. R. Williams, K. A. Slater, and E. D. Getzoff. 1994. Complete chemical structure of photoactive yellow protein: novel thioester-linked 4-hydroxycinnamyl chromophore and photocycle chemistry. *Biochemistry*. 33:14369–14377.
6. Meyer, T. E., G. Tollin, J. H. Hazzard, and M. A. Cusanovich. 1989. Photoactive yellow protein from the purple phototrophic bacterium, *Ectothiorhodospira halophila*. Quantum yield of photobleaching and effects of temperature, alcohols, glycerol, and sucrose on kinetics of photobleaching and recovery. *Biophys. J*. 56:559–564.
7. Meyer, T. E., G. Tollin, T. P. Causgrove, P. Cheng, and R. E. Blankenship. 1991. Picosecond decay kinetics and quantum yield of fluorescence of the photoactive yellow protein from the halophilic purple phototrophic bacterium, *Ectothiorhodospira halophila*. *Biophys. J*. 59:988–991.
8. Kim, M., R. A. Mathies, W. D. Hoff, and K. J. Hellingwerf. 1995. Resonance Raman evidence that the thioester-linked 4-hydroxycinnamyl chromophore of photoactive yellow protein is deprotonated. *Biochemistry*. 34:12669–12672.
9. Hoff, W. D., I. H. M. van Stokkum, H. J. van Ramesdonk, M. E. van Brederode, A. M. Brouwer, J. C. Fitch, T. E. Meyer, R. van Grondelle, and K. J. Hellingwerf. 1994. Measurement and global analysis of the absorbance changes in the photocycle of the photoactive yellow protein from *Ectothiorhodospira halophila*. *Biophys. J*. 67:1691–1705.
10. Takeshita, K., Y. Imamoto, M. Kataoka, K. Mihara, F. Tokunaga, and M. Terazima. 2002. Structural change of site-directed mutants of PYP: new dynamics during pR state. *Biophys. J*. 83:1567–1577.
11. Cusanovich, M. A., and T. E. Meyer. 2003. Photoactive yellow protein: a prototypic PAS domain sensory protein and development of a common signaling mechanism. *Biochemistry*. 42:4759–4770.
12. Losi, A., and S. E. Braslavsky. 2003. The time-resolved thermodynamics of the chromophore-protein interactions in biological photosensors as derived from photothermal measurements. *Phys. Chem. Chem. Phys*. 5: 2739–2750.
13. Harigai, M., Y. Imamoto, H. Kamikubo, Y. Yamazaki, and M. Kataoka. 2003. Role of an N-terminal loop in the secondary structural change of photoactive yellow protein. *Biochemistry*. 42:13893–13900.
14. Hendriks, J., T. Gensch, L. Hviid, M. A. van der Horst, K. J. Hellingwerf, and J. J. van Thor. 2002. Transient exposure of hydrophobic surface in the photoactive yellow protein monitored with Nile red. *Biophys. J*. 82: 1632–1643.
15. Hoff, W. D., A. Xie, I. H. M. van Stokkum, X.-J. Tang, J. Gural, A. R. Kroon, and K. J. Hellingwerf. 1999. Global conformational changes upon receptor stimulation in photoactive yellow protein. *Biochemistry*. 38:1009–1017.
16. Craven, C. J., N. M. Derix, J. Hendriks, R. Boelens, K. J. Hellingwerf, and R. Kaptein. 2000. Probing the nature of the blue-shifted intermediate of photoactive yellow protein in solution by NMR: hydrogen-deuterium exchange data and pH studies. *Biochemistry*. 39:14392–14399.
17. Van der Horst, M. A., I. H. Stokkum, W. Crielaard, and K. J. Hellingwerf. 2001. The role of the N-terminal domain of photoactive yellow protein in the transient partial unfolding during signaling state formation. *FEBS Lett*. 497:26–30.
18. Bernard, C., K. Houben, N. M. Derix, D. Marks, M. A. van der Horst, K. J. Hellingwerf, R. Boelens, R. Kaptein, and N. A. J. van Nuland. 2005. The solution structure of a transient photoreceptor intermediate: Δ25 photoactive yellow protein. *Structure*. 13:953–962.
19. Khan, J. S., Y. Imamoto, Y. Yamazaki, M. Kataoka, F. Tokunaga, and M. Terazima. 2005. A biosensor in the time domain based on the diffusion coefficient measurement: intermolecular interaction of an intermediate of photoactive yellow protein. *Anal. Chem*. 77:6625–6629.
20. Khan, J. S., Y. Imamoto, M. Harigai, M. Kataoka, and M. Terazima. 2006. Conformational changes of PYP monitored by diffusion coefficient: effect of N-terminal α-helices. *Biophys. J*. 90:3686–3693.
21. Takeshita, K., Y. Imamoto, M. Kataoka, F. Tokunaga, and M. Terazima. 2002. Thermodynamic and transport properties of intermediate states of the photocyclic reaction of photoactive yellow protein. *Biochemistry*. 41:3037–3048.
22. Imamoto, Y., H. Kamikubo, M. Harigai, N. Shimizu, and M. Kataoka. 2002. Light-induced global conformational change of photoactive yellow protein in solution. *Biochemistry*. 41:13595–13601.
23. Chen, E., T. Gensch, A. B. Gross, J. Hendriks, K. J. Hellingwerf, and D. S. Kliger. 2003. Dynamics of protein and chromophore structural changes in the photocycle of photoactive yellow protein monitored by time-resolved optical rotatory dispersion. *Biochemistry*. 42: 2062–2071.
24. Xie, A., L. Kelemen, J. Hendriks, B. J. White, K. J. Hellingwerf, and W. D. Hoff. 2001. Formation of a new buried charge drives a large-amplitude protein quake in photoreceptor activation. *Biochemistry*. 40: 1510–1517.
25. Nada, T., and M. Terazima. 2003. A novel method for study of protein folding kinetics by monitoring diffusion coefficient in time domain. *Biophys. J*. 85:1876–1881.
26. Eitoku, T., Y. Nakasone, D. Matsuoka, S. Tokutomi, and M. Terazima. 2005. Conformational dynamics of phototropin 2 LOV2 domain with the linker upon photoexcitation. *J. Am. Chem. Soc*. 127:13238–13244.
27. Nakasone, Y., T. Eitoku, D. Matsuoka, S. Tokutomi, and M. Terazima. 2006. Kinetic measurement of transient dimerization and dissociation reaction of *Arabidopsis* phototropin 1 LOV2 domain. *Biophys. J*. 91: 645–653.
28. Nakasone, Y., T. Eitoku, D. Matsuoka, S. Tokutomi, and M. Terazima. 2007. Dynamics of conformational changes of *Arabidopsis* phototropin 1 LOV2 with the linker domain. *J. Mol. Biol*. 367:432–442.
29. Nishida, S., T. Nada, and M. Terazima. 2004. Kinetics of intermolecular interaction during protein folding of reduced cytochrome *c*. *Biophys. J*. 87:2663–2675.
30. Nishida, S., T. Nada, and M. Terazima. 2005. Hydrogen bonding dynamics during protein folding of reduced cytochrome *c*: temperature and denaturant concentration dependence. *Biophys. J*. 89:2004–2010.
31. Hirota, S., Y. Fujimoto, J. Choi, N. Baden, N. Katagiri, M. Akiyama, R. Hulsker, M. Ubbink, T. Okajima, T. Takabe, N. Funasaki, Y. Watanabe, and M. Terazima. 2006. Conformational changes during apoplastocyanin folding observed by photocleavable modification and transient grating. *J. Am. Chem. Soc*. 128:7551–7558.
32. Terazima, M. 2006. Diffusion coefficients as a monitor of reaction kinetics of biological molecules. *Phys. Chem. Chem. Phys*. 8:545–557.
33. Terazima, M. 1998. Photothermal studies of photophysical and photochemical processes by the transient grating method. *In* Advanced Photochemistry. John-Wiley & Sons, New York
34. Terazima, M., and N. Hirota. 1993. Translational diffusion of a transient radical studied by the transient grating method, pyrazinyl radical in 2-propanol. *J. Chem. Phys*. 98:6257–6262.
35. Takeshita, K., N. Hirota, Y. Imamoto, M. Kataoka, F. Tokunaga, and M. Terazima. 2000. Temperature-dependent volume change of the initial step of the photoreaction of photoactive yellow protein (PYP) studied by transient grating. *J. Am. Chem. Soc*. 122:8524–8528.
36. Imamoto, Y., M. Harigai, and M. Kataoka. 2004. Direct observation of the pH-dependent equilibrium between L-like and M intermediates of photoactive yellow protein. *FEBS Lett*. 577:75–80.
37. Shimizu, N., Y. Imamoto, M. Harigai, H. Kamikubo, Y. Yamazaki, and M. Kataoka. 2006. pH-dependent equilibrium between long lived near-UV intermediates of photoactive yellow protein. *J. Biol. Chem*. 281: 4318–4325.
38. Harigai, M., M. Kataoka, and Y. Imamoto. 2006. A single CH/π weak hydrogen bond governs stability and the photocycle of the photoactive yellow protein. *J. Am. Chem. Soc*. 128:10646–10647.